

# Large time-step numerical modelling of the flow of Maxwell materials

*R.C. Bailey*

Geology and Physics Depts., University of Toronto,  
Toronto, Ontario M5S 1A7, Canada

August 1, 2003

*Maxwell viscoelastic materials are commonly simulated numerically in order to model the stresses and deformations associated with large-scale earth processes, such as mantle convection or crustal deformation. Both implicit and explicit time-marching methods require that the timesteps used be small compared with the Maxwell relaxation time if accurate solutions are to be obtained. For crustal tectonic modelling, where Maxwell times in a ductile lower crust may be of order of a decade or less, the large number of timesteps required to model processes lasting many millions of years imposes a huge computational burden. This burden is avoidable. In this paper I show that, with the appropriate formulation of the problem, timesteps may be taken which are much larger than the Maxwell time without loss of accuracy, as long as they are not large compared with the inverse strain rates (“tectonic” timescales) in the model. The method relies on explicit analytic integration of the Maxwell constitutive relation*

*for the stress over time intervals which may be longer than the relaxation time as long as they are short compared with the timescale over which crustal stresses and geometries change. The validity of the formulation is also demonstrated numerically with two simple models, one involving extension of a uniform block, and the other involving the shear of a composite layer.*

**Keywords:** Tectonic modelling - Maxwell - viscoelastic - large timesteps

# 1 Introduction

Earth processes which are represented by the behaviour of a viscoelastic solid [Ranalli 1995] are now routinely modelled numerically [Melosh & Raefsky 1980, Sabadini, Yuen & Portney 1986, Wu 1992, Komatitsch & Tromp 1999, Martinec 2000, Letychev *et al* 2001, Huismans *et al* 2001, Moresi *et al* 2001]. For tectonic modelling problems of slow processes involving the entire crust, however, the wide range of physically important timescales (Maxwell relaxation times alone span at least six orders of magnitude) makes accurate finite-element modelling difficult, or at the very least time consuming: for numerical stability, simple explicit time-marching of the Maxwell constitutive relation has to proceed with steps significantly less than the shortest relaxation time present in the modelled region. Approaches which use implicit methods avoid this stability problem: implicit methods are unconditionally stable for all timestep sizes. However, implicit methods are not accurate for timesteps comparable with the Maxwell relaxation time, so that small timesteps are desirable even for implicit methods. For hot lower crust in tectonically active regions, the viscosity  $\eta$  may be as low as  $10^{17}$  or  $10^{18}$  Pa-s [Klein *et al* 1997]. With a shear modulus  $\mu$  of 20 GPa, for example, this implies a Maxwell time  $\tau = \eta/\mu$  of the order of 10 years. This means a very large number of modelling steps are required to satisfy the timestep constraint above, even though it may take millions of

years for significant tectonic displacements to occur.

To illustrate the problem, consider the very simple case of stress decaying in a non-deforming block of a Maxwell material. The stress decays as  $\exp(-t/\tau)$  where  $\tau$  is the Maxwell time. Fig. 1 illustrates the problem: explicit methods of tracking Maxwell stress evolution of material with Maxwell relaxation time  $\tau$  effectively correspond to assuming a stress decay of the form  $(1 - t/\tau)$  and are only accurate for timesteps  $\Delta t \ll \tau$ . Implicit methods typically correspond to modelling the stress with a decay function of the form  $(1 + t/\tau)^{-1}$ , and are accurate at both short and long times, but not at intermediate times.

The requirement for short timesteps is frustrating when one realizes that stress and large-scale geometry in typical crustal tectonic processes change on a timescale (the “tectonic timescale”) much longer than the shortest Maxwell relaxation time present in the crust. This raises the possibility of using an implicit method and taking timesteps which are small compared to the tectonic timescale but large compared to the shortest relaxation times found in the crust, in order to accelerate the modelling computations. Because the relaxation times in the cold uppermost crust are always much longer than tectonic timescales, there must be somewhere in the model regions where the relaxation times will be comparable with the timestep, leading to the inaccuracies shown in Fig. 1 in this

region. If one judiciously chooses this timestep just small enough that this “difficult” region is sufficiently below the brittle ductile transition, where stresses are small and tectonically insignificant, then even large fractional errors in computing the stress there will not matter. Because stresses cannot adjust in the computation on timescales shorter than the timestep, this is equivalent to artificially increasing the viscosity (and thus the relaxation time) as far as possible in those parts of the model where it will make a negligible difference to the dynamics.

A better alternative is presented in this paper, in which the timestep may be chosen without worrying at all about the Maxwell relaxation time. The only constraint on this choice is that the timestep has to be small compared to the tectonic timescale (the inverse of the tectonic strain rate). This is not an onerous restriction; it is the same condition which must be applied in any case for Lagrangian mesh calculations in order to keep the mesh distortion per timestep small. Large timesteps are here dealt with by explicitly and analytically integrating the Maxwell constitutive relation for the stress over the timestep interval, on the assumption that the strain rate itself does not change significantly over the interval. The force-balance equation is also developed so as to be accurate over large timesteps. Finally, explicit numerical demonstrations of the method on two simple test cases are given.

## 2 Theory

### 2.1 Notation

The force balance or momentum equations for static or quasi-static problems (in which inertial terms are negligible) are given by

$$f_i + \frac{\sigma_{ij}}{\partial x_j} = 0 \quad (1)$$

where  $f_i$  is the  $i$ 'th component of the body force and  $\sigma_{ij}$  is the stress tensor. (The Einstein summation convention is used throughout.)

An isotropic linear elastic solid is described by

$$\sigma_{ij} = \lambda \epsilon_{kk} \delta_{ij} + 2\mu \epsilon_{ij} \quad (2)$$

where  $\lambda$  and  $\mu$  are the Lamé parameters. An isotropic linear viscous (Newtonian) fluid is described by

$$\sigma_{ij} = 2\eta \dot{\epsilon}_{ij} \quad (3)$$

where  $\eta$  is the viscosity. An isotropic linear viscoelastic (Maxwell) solid is described by

$$\dot{\sigma}_{ij}^{(D)} + \frac{\sigma_{ij}^{(D)}}{\tau} = 2\mu \dot{\epsilon}_{ij}^{(D)} \quad (4)$$

where the Maxwell relaxation time is defined as  $\tau = \eta/\mu$ , and the superscript  $^{(D)}$  indicates the deviatoric part of a tensor. On long timescales, this is the viscous relation, on short timescales, the deviatoric part of the elastic relation.

A constitutive relation which embodies Maxwell behaviour for deviatoric flow and elastic behaviour for dilatation is

$$2\mu\dot{\epsilon}_{ij} = \dot{\sigma}_{ij} + \frac{\sigma_{ij}^{(D)}}{\tau} - \frac{\lambda}{3K} \dot{\sigma}_{kk} \delta_{ij} \quad (5)$$

or

$$2\mu\dot{\epsilon}_{ij} = \dot{\sigma}_{ij} + \frac{\sigma_{ij}}{\tau} + \frac{p}{\tau} \delta_{ij} + \frac{\lambda}{K} \dot{p} \delta_{ij} \quad (6)$$

where  $p = -\sigma_{kk}/3$  is the pressure, and  $K = \lambda + 2\mu/3$  is the bulk modulus, defined by

$$K\theta = -p \quad (7)$$

for an elastic solid and  $\theta = \epsilon_{kk}$  is the dilatation.

## 2.2 Integrating the Maxwell constitutive relation

The Maxwell constitutive relation (4) can be quite generally integrated exactly to give

$$\sigma_{ij}^{(D)}(t) = \sigma_{ij}^{(D)}(0) + 2\mu \int_0^t e^{-t'/\tau} \dot{\epsilon}_{ij}^{(D)}(t') dt'. \quad (8)$$

If one assumes that the strain rate  $\dot{\epsilon}_{ij}^{(D)}$  is effectively constant over the (possibly large) interval  $\Delta t$ , (8) becomes

$$\sigma_{ij}^{(D)}(t + \Delta t) = \sigma_{ij}^{(D)}(t) e^{-\Delta t/\tau} + 2\eta \dot{\epsilon}_{ij}^{(D)} (1 - e^{-\Delta t/\tau}) \quad (9)$$

This relation, corresponding to the true decay curve in Fig. 1, is accurate no matter what the relaxation time is, as long as the timestep  $\Delta t$  is significantly shorter than the time over which the strain rate  $\dot{\epsilon}_{ij}^{(D)}$  changes significantly (the ‘‘tectonic’’ timescale). On its own,

however, it is useless unless the pressure and velocity fields can be solved for accurately over the same timestep (again assuming that the strain rates do not change significantly over that time).

The stress propagator equation (9) can if desired be written in terms of total rather than deviatoric stresses as

$$\sigma'_{ij} = (1 - s)(\sigma_{ij} + p\delta_{ij}) - p'\delta_{ij} + 2s\eta\dot{\epsilon}_{ij}^{(D)} \quad (10)$$

where the saturating growth function  $(1 - e^{-\Delta t/\tau})$  is abbreviated as  $s$ .

### 2.3 The large timestep force balance

The force balance equation at time  $t + \Delta t$  is exactly

$$0 = f_i(t + \Delta t) - \frac{\partial}{\partial x_i} p(t + \Delta t) + \frac{\partial}{\partial x_j} \sigma_{ij}^{(D)}(t + \Delta t) \quad (11)$$

Letting primes distinguish values at time  $t + \Delta t$  from variables evaluated at time  $t$  gives

$$0 = f'_i - \frac{\partial}{\partial x_i} p' + \frac{\partial}{\partial x_j} \sigma'_{ij}{}^{(D)} \quad (12)$$

With the same notation, the integrated deviatoric stress propagator (9) is

$$\sigma'_{ij}{}^{(D)} = \sigma_{ij}^{(D)} e^{-\Delta t/\tau} + 2\eta\dot{\epsilon}_{ij}^{(D)} (1 - e^{-\Delta t/\tau}) \quad (13)$$

or

$$\sigma'_{ij}{}^{(D)} = (1 - s)\sigma_{ij}^{(D)} + 2s\eta\dot{\epsilon}_{ij}^{(D)} \quad (14)$$

where the saturating growth function  $(1 - e^{-\Delta t/\tau})$  is abbreviated as  $s$ . Substituting (14) into (12) gives

$$0 = f'_i - \frac{\partial}{\partial x_i} p' + \frac{\partial}{\partial x_j} (1 - s)\sigma_{ij}^{(D)} + \frac{\partial}{\partial x_j} 2s\eta\dot{\epsilon}_{ij}^{(D)} \quad (15)$$

Alternatively, this can be written in terms of the total stress rather than the deviatoric stress: express the deviatoric stress in terms of the total stress:

$$\sigma_{ij}^{(D)} = \sigma_{ij} + p\delta_{ij} \quad (16)$$

and eliminate it from (15) to give

$$0 = f'_i - \frac{\partial}{\partial x_i} p' + \frac{\partial}{\partial x_j} (1 - s)(\sigma_{ij} + p\delta_{ij}) + \frac{\partial}{\partial x_j} 2s\eta\dot{\epsilon}_{ij}^{(D)} \quad (17)$$

Together with the dilatational part of the constitutive relation

$$-(p' - p) = k \dot{\epsilon}_{kk} \Delta t \quad (18)$$

this can be used to solve for the velocity field and the new pressure  $p'$  at the end of an arbitrarily large time interval  $\Delta t$  as long as the strain rate is effectively constant over that time interval. Together with the deviatoric stress propagator equation (9), equations (17) and (18) constitute a system for numerically solving a Maxwell viscoelastic deformation problem.

## 2.4 The equivalent Navier-Stokes problem

It is instructive to recast the system as an equivalent Navier-Stokes problem. Collecting terms with the aliases

$$f_i^{(E)} = f_i' + \frac{\partial}{\partial x_j} (1 - s)\sigma_{ij}^{(D)} \quad (19)$$

$$\eta^{(E)} = s\eta \quad (20)$$

restates equation (17) as a classic Navier-Stokes problem in terms of an effective body force  $f_i^{(E)}$ , an effective viscosity  $\eta^{(E)}$ , but the true pressure  $p'$  and strain-rate field  $\epsilon_{ij}^{(D)}$  as

$$0 = f_i^{(E)} - \frac{\partial}{\partial x_i} p' + \frac{\partial}{\partial x_j} 2\eta^{(E)}\dot{\epsilon}_{ij}^{(D)} \quad (21)$$

For timesteps  $\Delta t$  much larger than the Maxwell relaxation time, the effective viscosity is the true viscosity, and the behaviour modelled is that of a Newtonian viscous fluid. For timesteps  $\Delta t$  much shorter than the Maxwell relaxation time, the effective viscosity can be shown to be proportional to  $\Delta t$  (the stress rises linearly with time for constant strain rate), and equation (21) precisely models the elastic behaviour. At intermediate timestep sizes, the effective viscosity precisely models the intermediate behaviour.

The effective body force has, in addition to the true body force, a term which arises from differential unbalancing of the stress balance because of spatial gradients in the Maxwell relaxation time.

### 3 The Algorithm

The procedure for stepping forward in time is then seen to be, for a Lagrangian mesh formulation:

1. Compute the effective body force (19) using the true body force at time  $t + \Delta t$  and the stress tensor at time  $t$ ;
2. Solve the fictitious Navier-Stokes problem (21) (or its equivalent (17)) in conjunction with the dilatational equation (18) to obtain the true velocity field over the time interval  $\Delta t$ , and the new pressure  $p'$  at the end of that interval;
3. Use the integrated constitutive equation (10) to obtain the new deviatoric stress tensor  $\sigma'_{ij}$  at the end of the time interval  $\Delta t$ ;
4. Use the true velocity field to advect the mesh, problem boundaries, and any advected properties through the time interval  $\Delta t$ . If stress rotation is to be modelled (Jaumann stresses), the instantaneous rotation rate can be computed from the velocities and the stress tensor rotated at this point.

The formulation as an equivalent Navier-Stokes problem is convenient for intuiting the physics in terms of an effective viscosity, but not required for coding the problem. Equations (15) or (17) are equally well adapted to the direct implementation and the application of boundary conditions.

## 4 Plane strain tests of the algorithm

### 4.1 Coding platform

The algorithm was tested using a commercial PDE solver package (FEMLAB), modified to allow moving mesh (Lagrangian) solutions. Numerical solutions thus obtained for two representative plane-strain problems are presented here, along with the analytic solutions.

### 4.2 The plane strain Maxwell problem

The plane strain problem, although not as complicated as a full three-dimensional problem, is more complex for the viscoelastic case than for either the purely elastic or purely viscous cases, because the stress normal to the plane cannot be derived algebraically from other variables; it must be tracked as a time-dependent state variable by the PDE solver.

For displacements confined to the  $xy$  plane (so that  $\dot{\epsilon}_{zz} = \dot{\epsilon}_{xz} = \dot{\epsilon}_{zx} = 0$ ), no  $z$  directed body force, all quantities invariant with  $z$ , and zero shear stresses on the  $xy$  plane ( $\sigma_{xz} = \sigma_{yz} = 0$ ), the  $x$  and  $y$  components of equation (17) becomes

$$\begin{aligned}
 0 &= f_x + \frac{\partial}{\partial x} ((1-s)(\sigma_{xx} + p)) + \frac{\partial}{\partial y} ((1-s)\sigma_{xy}) \\
 &\quad - \frac{\partial}{\partial x} p' + \frac{\partial}{\partial x} \left( 2s\eta(\dot{\epsilon}_{xx} - \frac{1}{3}(\dot{\epsilon}_{xx} + \dot{\epsilon}_{yy})) \right) + \frac{\partial}{\partial y} (2s\eta\dot{\epsilon}_{xy}) \\
 0 &= f_y + \frac{\partial}{\partial y} ((1-s)(\sigma_{yy} + p)) + \frac{\partial}{\partial x} ((1-s)\sigma_{xy}) \\
 &\quad - \frac{\partial}{\partial y} p' + \frac{\partial}{\partial x} \left( 2s\eta(\dot{\epsilon}_{yy} - \frac{1}{3}(\dot{\epsilon}_{xx} + \dot{\epsilon}_{yy})) \right) + \frac{\partial}{\partial x} (2s\eta\dot{\epsilon}_{xy})
 \end{aligned} \tag{22}$$

The  $z$  component of equation (17) yields the identity  $0 = 0$ .

In purely elastic or purely viscous problems, the out-of-plane normal stress  $\sigma_{zz}$  implicit in  $p$  can be explicitly eliminated from the above equations by obeying the constraint  $\dot{\epsilon}_{zz} = 0$  in the constitutive equations. This is not possible here. Consider the  $zz$  component of the constitutive equations (6):

$$0 = 2\mu\dot{\epsilon}_{zz} = \dot{\sigma}_{zz} + \frac{\sigma_{zz}}{\tau} + \frac{p}{\tau} + \frac{\lambda}{K}\dot{p} \quad (23)$$

For fast variations (compared to  $\tau$ ), elastic behaviour prevails and

$$0 = \dot{\sigma}_{zz} + \frac{\lambda}{K}\dot{p} = \dot{\sigma}_{zz} - \frac{\lambda}{3K}(\dot{\sigma}_{xx} + \dot{\sigma}_{yy} + \dot{\sigma}_{zz}) \quad (24)$$

yielding

$$\sigma_{zz} = -\frac{p}{1 + \frac{2\mu}{3\lambda}} = \frac{\lambda}{2(\lambda + \mu)}(\sigma_{xx} + \sigma_{yy}) \quad (25)$$

For slow variations, viscous behaviour prevails and

$$0 = \dot{\sigma}_{zz} + \frac{\lambda}{K}\dot{p} = \dot{\sigma}_{zz} - \frac{\lambda}{3K}(\dot{\sigma}_{xx} + \dot{\sigma}_{yy} + \dot{\sigma}_{zz}) \quad (26)$$

yielding

$$\sigma_{zz} = \frac{\lambda}{3K - \lambda}(\sigma_{xx} + \sigma_{yy}). \quad (27)$$

In a general plane-strain viscoelastic problem, however,  $\sigma_{zz}$  cannot be explicitly eliminated in this way. It, or equivalently the pressure  $p$ , must be explicitly tracked with (23) or (7).

## 5 An extensional test

This describes a test using plane strain unconfined uniaxial extension. Although very simple, it is sufficient to demonstrate that the

solution formulation is stable and accurate, and uses mixed kinematic and stress boundary conditions. In this test, a rectangular prism of y-height  $h$  and x-width  $w$ , of infinite extent in the z-direction, is uniaxially extended in the y-direction. Beginning with a stress-free state at time zero, the top is pulled upward at velocity  $v_0$ , the bottom being held fixed. The material is unconfined in the x-direction, so that normal stresses applied to the x-sides are zero. Strain  $\epsilon_{zz}$  in the z-direction is also kept to zero, so that this is a plane strain solution. Tangential stresses on all boundaries are zero. No body force is present. Although a solution is here presented for one prism, this is also a valid solution for an arbitrary number of such prisms, of different mechanical properties, stacked beside each other in a composite block, since the side boundary conditions are identical for all the prisms.

Strain and stress rates are uniform within the prism. The prism's sides are coincident with the principal axes of stress and strain, so that  $\sigma_{xy} = \dot{\epsilon}_{xy} = 0$ . The boundary conditions force  $\sigma_{xx} = 0$ . The vertical strain rate is prescribed: the thickness  $h$  will change with time as  $h(t) = h_0 + v_0 t$ , so that the strain rate is time-dependent as

$$\dot{\epsilon}_0 = v_0/h = \frac{v_0}{h_0 + v_0 t} \quad (28)$$

This can more simply be written in terms of the characteristic strain time (the “tectonic” timescale)  $\tau_c = h_0/v_0$  (which will be negative

for compressional straining) as

$$\dot{\epsilon}_0(t) = v_0/h = \frac{1}{\tau_c + t}. \quad (29)$$

The pressure variation can be shown to be

$$p(t) = -2\mu \frac{\tau}{\tau_p} e^{-(t+\tau_c)/\tau_p} \left[ \text{Ei} \left( \frac{t + \tau_c}{\tau_p} \right) - \text{Ei} \left( \frac{\tau_c}{\tau_p} \right) \right] \quad (30)$$

where Ei is the exponential integral function and

$$\tau_p = \tau \left( 1 + \frac{4\mu}{3K} \right). \quad (31)$$

Fig. 2 shows a comparison of the numerical model of this extension with the theoretical solution (30). The tension (negative pressure) builds linearly initially as the material behaves elastically. At longer times, the behaviour is viscous, with tension proportional to strain rate (because the velocity is constant, the strain rate falls off as the elongation becomes significant).

## 6 A shear test

A more complex shear deformation test is described here, which tests most of the relevant physics of the above formulation of a Maxwell solver, but in particular adds the modelling of the differential relaxation term contribution to the effective body force (19). Consider a body made of two welded blocks of heights  $a$ ,  $b$  in the  $y$  direction, and infinite width in the  $x$  direction, consisting of an top block of properties  $\mu_1$  and  $\eta_1$ , and a bottom block of properties  $\mu_2$  and  $\eta_2$ .

Let the weld plane be at  $y = 0$ . From a state of zero stress, constant velocity boundary conditions for the horizontal velocity  $u$  ( $u = V_t$  and  $u = V_b$  at top and bottom respectively) are switched on at time zero. This drives simple shear involving horizontal motion only.

The motion of points on the boundary is in general time dependent: consider, for example, the case where  $\mu_b \gg \mu_t$  and  $\eta_b \ll \eta_t$ , so that the lower block is elastically stiff but relaxes quickly, and the upper block is elastically soft but relaxes slowly. Initially, shear strains will build up linearly with time in both blocks, but the lower block will elastically resist shearing much more than the upper, with strain a factor  $\mu_t/\mu_b$  less than that of the lower block. Points on the boundary between the blocks will move leftwards from their initial positions (negative velocity), carried by the lower block's initial refusal to deform very much. As stress builds up, a higher fraction of the strain will be viscous shear, and the upper persistent block will strain more slowly than the lower one. The upper block will then drag the boundary with it, leading to a reversal in the boundary velocity. A detailed analysis gives, for the boundary velocity

$$V_0(t) = h\dot{\epsilon}_0 \left[ \frac{\eta_0}{\eta_\Delta} + \left( \frac{\mu_0}{\mu_\Delta} - \frac{\eta_0}{\eta_\Delta} \right) e^{-\frac{t}{\tau_0}} \right] \quad (32)$$

where mean properties  $\mu_0$ ,  $\eta_0$  and  $\tau_0$  are defined by

$$\frac{1}{\mu_0} = \frac{a/h}{\mu_t} + \frac{b/h}{\mu_b} \quad (33)$$

$$\frac{1}{\eta_0} = \frac{a/h}{\eta_t} + \frac{b/h}{\eta_b} \quad (34)$$

$$\tau_0 = \frac{\eta_0}{\mu_0} \quad (35)$$

and differential properties  $\mu_\Delta$  and  $\eta_\Delta$  are defined by

$$\frac{1}{\mu_\Delta} = \frac{b/h}{\mu_b} - \frac{a/h}{\mu_t} \quad (36)$$

and

$$\frac{1}{\eta_\Delta} = \frac{b/h}{\eta_b} - \frac{a/h}{\eta_t} \quad (37)$$

By integrating this with respect to time, we can get the x-displacement of a particle on the welded boundary as a function of time:

$$X_0(t) = h\dot{\epsilon}_0 \left[ \frac{\eta_0}{\eta_\Delta} t + \tau_0 \left( \frac{\mu_0}{\mu_\Delta} - \frac{\eta_0}{\eta_\Delta} \right) (1 - e^{-\frac{t}{\tau_0}}) \right] \quad (38)$$

Fig 3 shows a comparison between this equation and a numerical computation using the algorithm outlined in this paper. The model's relaxation times span four orders of magnitude; the numerical timestep used is ten times the smallest relaxation time. The computation accurately tracks the time-dependent behaviour predicted by Eq. (38).

## 7 Errors

The errors for large timesteps are qualitatively described by Fig. (1); the explicit method is unstable and it is clear that the implicit method can have significant errors at intermediate timestep sizes. The errors of the different methods of propagating the stress forward in time can be examined more quantitatively by comparing them to

the full solution using the general integral (8). An arbitrary strain rate is represented as a power series in time as

$$\dot{\epsilon}(t) = \dot{\epsilon}_0 + \dot{\epsilon}_1 t + \frac{1}{2}\dot{\epsilon}_2 t^2 + \dots \quad (39)$$

where the coefficients  $\dot{\epsilon}_0, \dot{\epsilon}_1, \dot{\epsilon}_2, \text{etc.}$  are constant in time. Substitution of (39) into (8) and integrating explicitly yields

$$\begin{aligned} \sigma(t) = & \sigma(0)e^{-t/\tau} + 2\mu\tau(1 - e^{-t/\tau})\dot{\epsilon}_0 + \\ & 2\mu\left(\tau^2(1 - e^{-t/\tau}) - \tau t e^{-t/\tau}\right)\dot{\epsilon}_1 + \dots \end{aligned} \quad (40)$$

It is more useful to represent each of the strain rate coefficients in terms of a corresponding time-scale  $\dot{\epsilon}_n = T_n^{n+1}$ , where the timescale constants  $T_n$  are all of the order of the “tectonic” timescale, the time over which the strain rate changes significantly. (For example, explicit differentiation of the strain rate in the extensional test above yields  $|T_n| = T_0 = \dot{\epsilon}_0^{-1}$  for all  $n$ ). Then

$$\begin{aligned} \sigma(t) = & \sigma(0)e^{-t/\tau} + 2\mu\frac{\tau}{T_0}(1 - e^{-t/\tau}) + \\ & 2\mu\left(\frac{\tau^2}{T_1^2}(1 - e^{-t/\tau}) - \frac{\tau t}{T_1^2}e^{-t/\tau}\right) + \dots \end{aligned} \quad (41)$$

The stresses predicted by the explicit method, implicit method, and the method developed here are, respectively

$$\sigma_E(t) = \sigma(0) + 2\mu\frac{t}{T_0} \quad (42)$$

$$\sigma_I(t) = \sigma(0) + 2\mu \left( \frac{1}{1 + t/\tau} \right) \frac{t}{T_0} \quad (43)$$

$$\sigma_H(t) = \sigma(0)e^{-t/\tau} + 2\mu(1 - e^{-t/\tau})\frac{\tau}{T_0} \quad (44)$$

For timesteps small compared to the relaxation time  $\tau$ , all of the methods are accurate and stable. We are interested in timesteps which are significantly larger than  $\tau$ , but of course significantly smaller than the tectonic timescales  $T_0$ ,  $T_1$ , *etc.*. As timestep size becomes large compared to  $\tau$ , the relative errors tend to infinity for the unstable explicit method. For both the implicit method and the method here, they tend to a small value (not zero unless  $\dot{\epsilon}$  is constant). As a fraction of the true stress change  $\Delta\sigma = \sigma(\Delta t) - \sigma(0)$ , the errors of the two methods have a term of order

$$\frac{\delta\sigma_I}{\Delta\sigma} \sim \frac{\tau}{T_1} + \frac{\tau}{\Delta t} \quad (45)$$

and

$$\frac{\delta\sigma_H}{\Delta\sigma} \sim \frac{\tau}{T_1} \quad (46)$$

The implicit method has an additional term of order  $\tau/\Delta t$  which can be significantly larger than  $\tau/T_1$  for timesteps larger than  $\tau$ ; the difference between the two methods can be of order 25%.

There are situations in which the larger relative errors of the implicit method do not matter. To be more specific, consider the Earth's crust: hot and weak (low viscosity and relaxation times as low as ten years) at depth, but cool and strong (high viscosity

and relaxation times which may be as high as  $10^8$  years) near the surface. Many tectonic phenomena of interest occur on timescales intermediate between these limits. For the lower crust, these tectonic timescales are so long that no significant deviatoric stresses accumulate, and the large relative error of the implicit method does not matter. For the strong upper crust, the tectonic timescales are so short compared to the relaxation time that the errors for all the methods are small in an absolute sense. Only if the details of the stress accumulation and dissipation in the intermediate crust are important will the implicit method fail to be useful. An example of such a situation would be in attempts to predict the depths to which brittle faulting could occur during a particular tectonic deformation; as implied by Fig. (1), the implicit method would retain a significantly larger fraction of accumulating stresses than the true method; it would predict significantly greater depths. More generally, any modelling of processes sensitive to the location of or rate of the transformation from ductile physics to brittle physics would be better done by the method presented here, if large timesteps are to be taken.

## References

[Huisman *et al* 2001] Huisman RS, Podladchikov YY, Cloetingh S., Transition from passive to active rifting: Relative importance

of asthenospheric doming and passive extension of the lithosphere, *J. Geophys. Res. - Solid Earth* , **106**, 11271-11291.

[Klein *et al* 1997] Klein, A., W. Jacoby and P. Smilde, Mining Induced Crustal Deformation in Northwest Germany: Modeling the Rheological Structure of the Lithosphere, *Earth and Planetary Science Letters*, **147**, 107-123.

[Komatitsch & Tromp 1999] Komatitsch, D. & Tromp, J., Introduction to the spectral-element method for 3-D seismic wave propagation, *Geophys. J. Int.*, **139**, 806-822.

[Latychev *et al* 2001] Latychev, K., Tromp, J., Tamisea, M., Mitrovica, J.& Komatitsch, D., Modeling the response of a three-dimensional viscoelastic Earth, *Eos Trans. AGU*, **82**(47), Fall Meet. Suppl., Abstract T42F-10.

[Martinec 2000] Martinec, Z., Spectral-finite element approach to three-dimensional viscoelastic relaxation in a spherical earth, *Geophys. J. Int.*, **142**, 117-141.

[Melosh & Raefsky 1980] Melosh, H.J. & Raefsky, A., The dynamical origin of subduction zone topography, *Geophys. Jour. R. Astr. Soc.*, **60**, 333-354.

[Moresi *et al* 2001] Moresi, L. Mühlhaus, H.-B. & Dufour, F., Viscoelastic formulation for modelling of plate tectonics, in *Bifurca-*

*tion and Localization in soils and Rocks 99*, Mühlhaus, Dyskin, A. and Pasternak, E. (eds.), Balkema: Rotterdam.

[Ranalli 1995] Ranalli, G., *Rheology of the Earth*, 2nd Ed., Chapman and Hall, London, 413 pp.

[Sabadini, Yuen & Portney 1986] Sabadini, R., Yuen, D.A. & Portney, M., 1986. The effects of upper-mantle lateral heterogeneities on postglacial rebound, *Geophys. Res. Lett.*, **13**, 337-340.

[Wu 1992] Wu, P., Deformation of an incompressible viscoelastic flat earth with Power Law Creep: a Finite Element approach, *Geophys. J. Int.*, **108**, 136-142.

## Figure Captions

Figure 1: Computed decays of elastic stress in a non-deforming Maxwell solid with unit Maxwell relaxation time: dot-dash curve: explicit methods; dashed curve: implicit methods; solid curve: true decay.

Figure 2: Variation of pressure in a homogenous block, initially a unit square. The viscosity is 1, the shear and bulk moduli are 1 and 2, respectively. The lower face of the block is fixed, the top forced to extend at a constant velocity of 0.0025, for a tectonic timescale of order 400. The top and bottom faces have zero tangential stresses applied, and the side faces of the block are both normal- and tangential-stress free. The total strain rate thus varies inversely with the length of the block. The Maxwell time is unity. The solid line is the theoretical result from Eq. (30). The circles are the computed values using a timestep of 2.5, significantly larger than the Maxwell relaxation time. The computational mesh elements used were about 20% of the block thickness. Errors are of the order of a percent or so as suggested by equation (46).

Figure 3: Variation of position of a point (initially at  $x = 0.03$ ,  $y = 0$ ) on the boundary between two welded homogenous layers, each of unit thickness. The total strain rate averaged across the two layers is forced to be 0.1. The Maxwell time is 100 in the top layer ( $\mu = 0.1$ ,  $\eta = 10$ ) and 0.01 in the bottom layer ( $\mu = 10$ ,  $\eta = 0.01$ ). The solid line is the theoretical result from Eq. (38). The circles are the computed values using a timestep of 0.1, one order of magnitude larger than the Maxwell relaxation time in the lower layer. The computational mesh elements used were about 20% of the layer thickness. The magnitude of the errors is consistent with that suggested by (46).

...

Figure 1

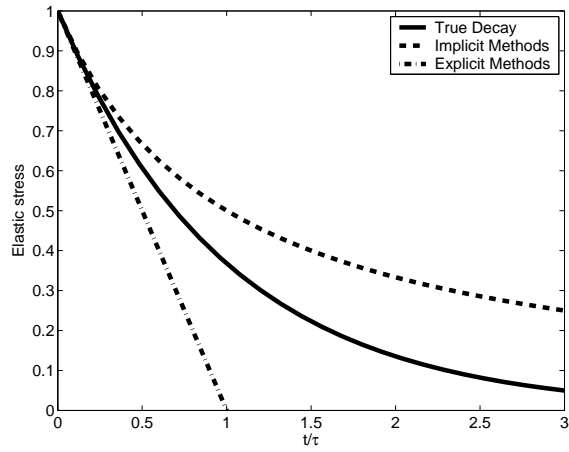


Figure 2

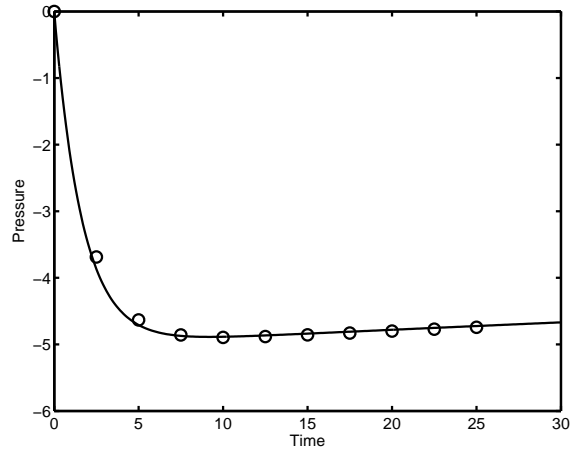


Figure 3

